

## A Possible Relationship between Deep Earthquakes and the Structural Transition of Submolecular SiO<sub>2</sub> Fragments in Rocks of a Subducting Oceanic Slab

M.I. Kuzmin<sup>a,✉</sup>, R.G. Khlebopros<sup>b,d,†</sup>, A.N. Didenko<sup>c,e</sup>, S.G. Kozlova<sup>f,g</sup>, V.E. Zakhvataev<sup>b,d</sup>

<sup>a</sup> A.P. Vinogradov Institute of Geochemistry, Siberian Branch of Russian Academy of Sciences, ul. Favorskogo 1A, Irkutsk, 664033, Russia

<sup>b</sup> Federal Research Center Krasnoyarsk Scientific Center, Siberian Branch of the Russian Academy of Sciences, Akademgorodok 50, Krasnoyarsk, 660036, Russia

<sup>c</sup> Yu.A. Kosygin Institute of Tectonics and Geophysics, Far Eastern Branch of the Russian Academy of Sciences, ul. Kim Yu Chena 65, Khabarovsk, 680000, Russia

<sup>d</sup> Siberian Federal University, pr. Svobodnyi 78, 660041, Krasnoyarsk, Russia

<sup>e</sup> Pacific National University, ul. Tikhookeanskaya 136, Khabarovsk, 680035, Russia

<sup>f</sup> A.V. Nikolaev Institute of Inorganic Chemistry, Siberian Branch of the Russian Academy of Sciences, pr. Akademika Lavrent'eva 3, Novosibirsk, 630090, Russia

<sup>g</sup> V.G. Shukhov Belgorod State Technological University, ul. Kostyukova 46, Belgorod, 308012, Russia

Received 22 May 2018; received in revised form 11 July 2018; accepted 26 July 2018

**Abstract**—Quantum-chemical calculations show a tendency of SiO<sub>2</sub> molecule to transform from linear to isomeric cyclic (bent) form and back. In the latter case, the energy released during the transition isomeric SiO<sub>2</sub> → linear SiO<sub>2</sub> is about 240 kJ/mole. This hypothetical structural transition of submolecular SiO<sub>2</sub> fragments in mantle minerals is supposed to initiate deep-focus high-energy earthquakes at the upper–lower mantle boundary. It is at this depth (600–670 km) that the subducting oceanic slab is delaminated: Its upper part moves “horizontally” along the upper–lower mantle boundary, while its lower part separated into blocks subsides into the lower mantle and reaches the D” layer to accumulate there.

**Keywords:** phase transition, deep-focus earthquakes, upper–lower mantle, lithospheric plate, subduction

### INTRODUCTION

A remarkable deep earthquake, that appeared to be the largest deep-focus earthquake ever recorded by modern seismology (Fig. 1) occurred on May 24, 2013 beneath the Sea of Okhotsk near the Kamchatka Peninsula. It was felt as M2 event even at a distance of 6400 km in the European part of the Eurasia continent (Finland) (Tatevossian et al., 2014). The Okhotsk earthquake provoked a new wave of interest towards the mechanisms of deep earthquakes worldwide (Chebrov et al., 2013, 2015; Wei et al., 2013; Ye et al., 2013; Meng et al., 2014; Shestakov et al., 2014; Zhan et al., 2014; Chen and Wen, 2015; Voronina, 2016; Varga et al., 2017; and other).

Depending on the hypocenter depth all earthquakes are divided into three categories: earthquakes with a focal depth ranging from 0 to 70 km below the surface; events with focal depth of 70–300 km; and those whose focal depth exceeds 300 km. There are only two areas in Russia, which are

vulnerable to earthquakes occurring at a depth of over 300 km: (1) close to Vladivostok where deep-focus earthquakes are generated both on continents and in the Sea of Japan; (2) stretches in the northeast-southwestern direction from the western coastlands of Kamchatka Peninsula through Sakhalin Island and Tatarsky Strait in the Sea of Okhotsk to the coastline of Eurasia (Fig. 1).

The nature of deep-focus earthquakes has been a paradox since their discovery in the 1920s (Turner, 1922). There is a common viewpoint amongst geologists that most deep-focus earthquakes mainly occur in active subduction zones. However, the physics of their mechanisms is still a mystery as the temperature and pressure at these depths could inhibit accumulation of elastic strain energy in rocks which in turn prevents the subsequent brittle fracture of rocks thus generating earthquakes (e.g., Zharkov, 2013).

Deep-focus earthquakes make up only a small proportion (a few percent) of global seismic activity. However, they are of great significance as they bear direct information about the subducting lithosphere. It is known that oceanic slabs subduct much faster as compared with the time required for the subducting lithosphere to reach the temperature of the surrounding mantle. They remained “cold” and dense as

✉ Corresponding author.

E-mail address: mikuzmin@igc.irk.ru (M.I. Kuzmin)

† Deceased.

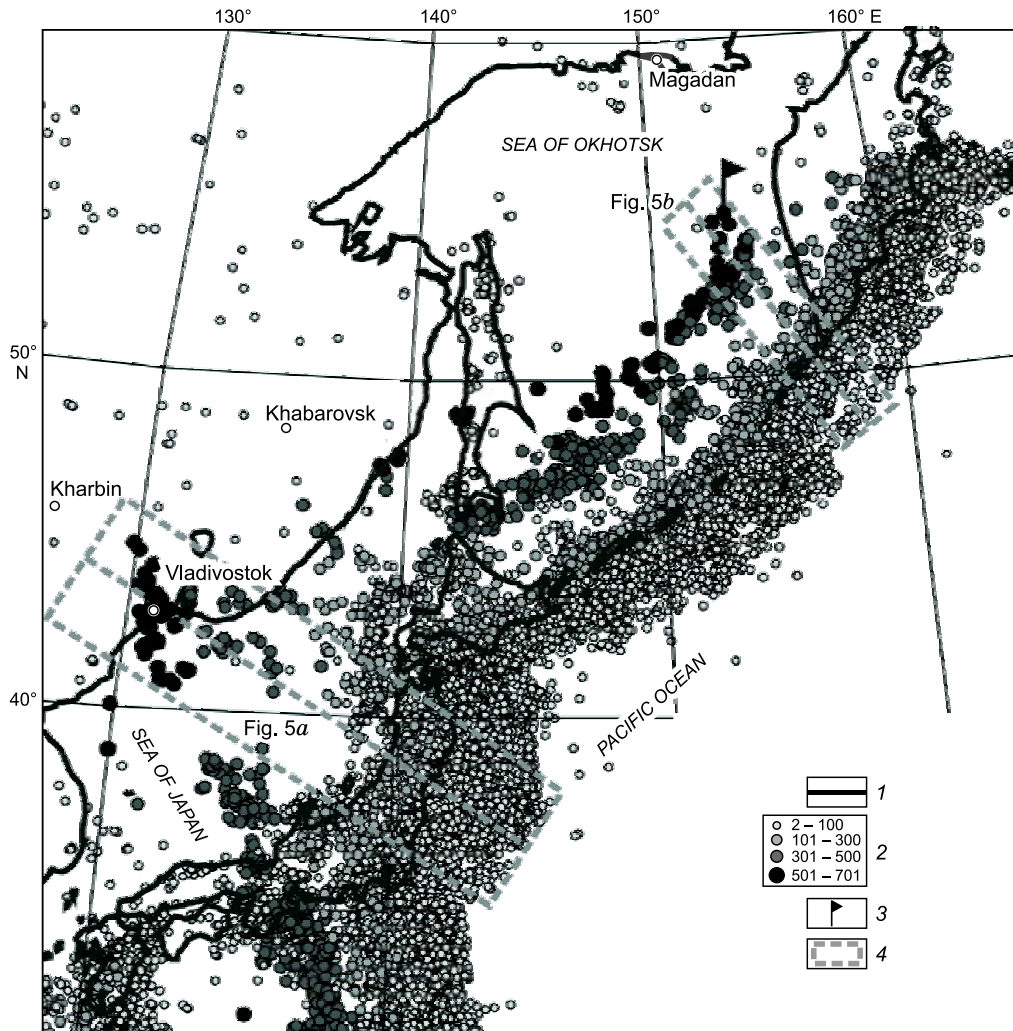


**Fig. 1.** Distribution of earthquakes ( $M \geq 4.5$ ) around the Kurile–Kamchatka and Japan island arcs. Catalog of earthquakes, US Geological Survey <https://earthquake.usgs.gov/earthquakes/search/>, 1900.07.29–2017.10.27. Azimuth equidistant projection, central meridian of 145° E. 1, coastline; 2, earthquakes and the intervals of their hypocenter depth; 3, Okhotsk Sea earthquake of May 24, 2013; 4, band synthesized profiles of the earthquake hypocenter depths shown in Fig. 5.

compared with “normal” mantle (Zonenshain and Kuzmin, 1993; Kirby et al., 1996; Frohlich, 2006).

Three models of physical-chemical processes occurring in the lower mantle are used to explain the nature of deep-focus earthquakes (Frohlich, 2006; Lyskova, 2014):

Dehydration of water-containing minerals, formed as a result of seafloor serpentinization of mantle ultramafic rocks (e.g., Pechersky et al., 1993) within the subducting slab. The presence of subduction-zone water can account for brittle rupture processes at lower shear stresses (Meade and Jeanloz, 1991), and thus can trigger deep-focus earthquakes.

Melting of rocks causing slip along shear zones owing to heat accumulation is expected to induce the explosive temperature increase that in turn triggers shear instability (Ogawa, 1987) being the cause of deep-focus earthquakes.

Polymorphic phase transformation of metastable olivine into spinel close to shear surface in the subducting lithosphere is suggested to cause the decrease in the rock hard-

ness due to changes of crystalline structure thus inducing deep-focus earthquakes. Such a mechanism can account for the earthquakes in the transition mantle zone (Kirby, 1987; Kirby et al., 1996).

There are, however, drawbacks to using of these above three models to explain the nature of deep-focus earthquakes: (1) the dehydration mechanism can hardly explain the nature of earthquakes with the hypocenter depth exceeding 300 km; (2) the mechanism of thermal shear instability is a mathematical model, there is no experimental (laboratory) evidence of brittle rupture process induced by shear melting; (3) the olivine-spinel phase transition at a depth of 600–700 km would require the decrease in temperature within the subducting slab by at least 250–300 °C as compared to the surrounding “normal” mantle. Such a critical analysis of available hypotheses describing the nature of deep-focus earthquakes is beyond the scope of this article.

The most obvious indication for the existence of relationships between deep-focus earthquakes and phase transitions in the upper mantle is the dependence of earthquake frequency on the depth (Rodkin and Rundkvist, 2017): the maximum in earthquake frequency is found close to boundaries of the supposed solid-solid phase transitions in the PREM (Preliminary Reference Earth Model) model (Dziewonski et al., 1975, 1981; Zharkov, 2013; and other). Shear instability models explain the shear movements in epicenters. Further studies concerning the mechanisms to generate deep-focus earthquakes are to combine positive components of these two approaches (Rodkin and Rundkvist, 2017).

This study focuses on structural transitions in mantle minerals containing submolecular SiO<sub>2</sub> fragments which could be an alternative mechanism in initiating deep-focus earthquakes. An increase in the temperature and pressure with depth leads to transformations of crystal lattices, atomic positions, bonds and distances between atoms in the mantle minerals (Pushcharovky and Oganov, 2006). Silica undergoes an intensive polymorphic transformation at high pressures. At relatively low pressures Si atom shows tetrahedral coordination with oxygen atoms attached in polymorphs in the form of silicon dioxide. At a pressure higher than 10 GPa each silicon atom becomes six-coordinated thus forming a new silica modification with the rutile structure which was named stishovite. In stishovite, the linear O=Si=O groups are connected with the same four bonds of Si...O coordination type. A series of poststishovite structural phase transitions have been identified: those with a CaCl<sub>2</sub>-type, α-PbO<sub>2</sub>-type, PbO<sub>2</sub>-type, ZrO<sub>2</sub>-type, α-PbCl<sub>2</sub>-type phases, etc. (Pushcharovsky and Oganov, 2006). Experimental and theoretical studies indicate that the second-order transition from stishovite to CaCl<sub>2</sub>-type structure occurs at a pressure of about 70 GPa and temperature of 1600 K (Kingma et al., 1995). It was also shown that at about 121 GPa and 2400 K the CaCl<sub>2</sub>-type silica undergoes further structural transition to a α-PbO<sub>2</sub> phase (Dubrovinsky et al., 1997) which in turn transforms to the phase with pyrite structure at a pressure exceeding 200 GPa (Kuwayama et al., 2005). There are some metastable phases of silicon dioxide at a pressure lower than 120 GPa (Pushcharovsky and Oganov, 2006). One of the local seismic discontinuities is attributed to the formation of stishovite. High-pressure phases of SiO<sub>2</sub> can be formed in small quantities in the mantle transition zone located at a depth between 410 and 670 km. It has been suggested that stishovite could be possibly formed in the Earth's mantle to the depth of at least 1200 km (Condie, 2011). From a depth of 1500 km stishovite transforms into the CaCl<sub>2</sub>-structured polymorph and then respectively from about 2300 km a new phase with PbCl<sub>2</sub> structure becomes stable.

Based on the hypothesis advanced in (Gabuda and Kozlova, 2009), it has been proposed that at higher pressures like those existing in the Earth's mantle (at a depth of about 1000 km) submolecular SiO<sub>2</sub> fragments could undergo a

transition from the linear structure to isomeric bent (cyclic) form (Zyubina et al., 1998; Mück et al., 2012; Zhao et al., 2014). Such a hypothetical transition might be of great importance for phase instability of some mantle minerals, like stishovite, and correspondingly for physical processes occurring in the Earth's mantle. Silicon is the most abundant element found in the Earth's mantle and, at the same time, the energy released during the transition from bent SiO<sub>2</sub> structure to linear SiO<sub>2</sub> structure is relatively large (about 2.5 eV or 4000 kJ/kg). A possible impact of such hypothetical structural phase transition of SiO<sub>2</sub> fragments on the dynamic processes in mantle melts was assessed in (Khleborpos et al., 2016, 2017). This study being a continuation of previous investigations by R.G. Khleborpos and a team, seeks to propose a possible mechanism for initiating deep-focus mantle earthquakes in subduction zones taking into account this structural transition.

### BENT (CYCLIC) SiO<sub>2</sub> FORM: HYPOTHETIC STRUCTURE OF CRYSTALS

The transition between the linear and cyclic isomers of SiO<sub>2</sub> is revealed in the quantum chemical calculations as the corresponding stable energy minima of SiO<sub>2</sub> molecule in the series of AB<sub>2</sub> molecules (A=C, Si, Ge, Sn, Pb and B=O, S, Se) (Zyubina, 1998; Gabuda et al., 2009; Mück et al., 2012; Zhao et al., 2014). Though the bent structure for SiO<sub>2</sub> is not experimentally accessible so far, the bent (cyclic) SiS<sub>2</sub> has been experimentally detected in the gas phase (Mück et al., 2012). The hypothetical bent SiO<sub>2</sub> structure can be obtained taking into account that the electron localization function (ELF) could be similar for hypothetical TeO<sub>2</sub> and SiO<sub>2</sub> molecules having a bent form (Fig. 2) (Gabuda et al., 2009). Both hypothetical TeO<sub>2</sub> and SiO<sub>2</sub> molecules are characterized by a similar number of monosynaptic basins (Silvi and Savin, 1994) of electron localization (ELF > 0.75): there is one basin on tellurium and silica atoms and there are two basins on each oxygen atom. In addition, both molecules are marked by similar ELF distribution on O–O lines. Such a stereochemical feature on cations was described by (Belov et al., 1982) as a localization of lone electron pair.

As regards the structure, TeO<sub>2</sub> paratellurite (β-TeO<sub>2</sub>) contains four coordinate tellurium supplemented by a lone electron pair (LP1) to trigonal bipyramid (Belov et al., 1982). The crystal structure of paratellurite is built up from {Te–O<sub>4</sub>} polyhedra. However, if one considers the tellurium atom to be linked to two nearest oxygen atoms, submolecular fragment TeO<sub>2</sub> with Te–O distance of 1.903 Å, ∠O–Te–O as 102° and LP1 on tellurium atom could be isolated (Belov et al., 1982). It has to be noted that geometry parameters of submolecular TeO<sub>2</sub> fragment in the paratellurite structure agrees well with the calculated data for a hypothetical TeO<sub>2</sub> molecule (calculated Te–O distance = 1.834 Å and ∠O–Te–O = 112°). Moreover, LP1 occurs both in submolecular TeO<sub>2</sub> fragments and a hypothetical bent TeO<sub>2</sub> molecule.

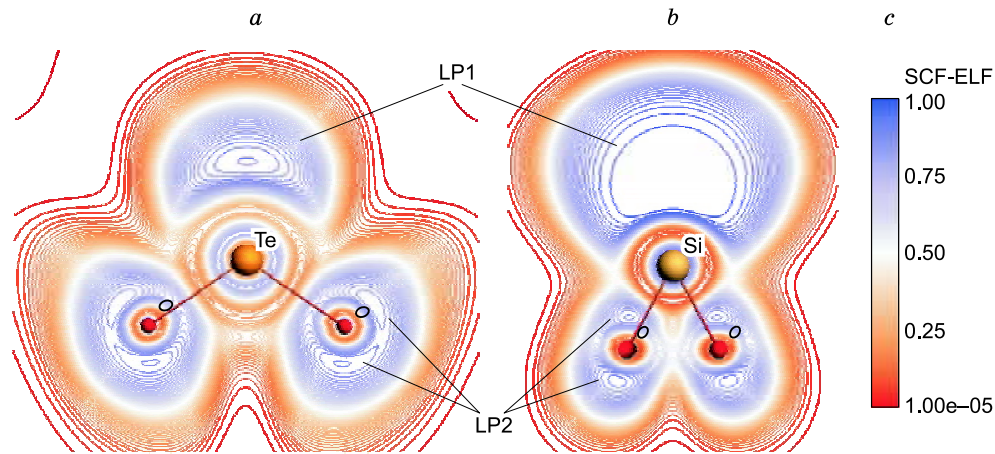


**Fig. 2.** The electron localization function (ELF) distributions are shown in the plane of the hypothetical molecules  $\text{TeO}_2$  (a) and  $\text{SiO}_2$  (b). The numerical values of the ELF are presented by colored contours, and the ELF maximum corresponds to blue, the minimum to red (c). LP1, 2 are lone electronic pairs. The calculation was carried out using the density functional theory method (VWN & BP/TZP) (Gabuda and Kozlova, 2009).

Thus, following similar ELF distribution for bent-shaped  $\text{TeO}_2$  and  $\text{SiO}_2$  molecules, it can be suggested that the hypothetical crystal structure with  $\text{SiO}_2$  cyclic form could resemble the paratellurite ( $\beta\text{-TeO}_2$ ) structure in the tetragonal synchony ( $P 4_12_12$  and  $Z = 4$ ). The geometry of a submolecular  $\text{SiO}_2$  fragment in the  $\beta\text{-SiO}_2$  structure could be different from the calculated parameters (distance for Si–O bonds = 1.687 Å and  $\angle\text{O–Si–O} = 57^\circ$ ). However, the LP1 position should change the coordination number of Si atoms and thus new bonds could be expected. In addition, other structural  $\text{SiO}_2$  modifications (e.g.,  $\alpha\text{-SiO}_2$ , similar to  $\alpha\text{-TeO}_2$ ) are possible as well as including liquid silica, consisting of corner  $\text{SiO}_2$  molecules.

## SPATIAL DISTRIBUTION OF DEEP-FOCUS EARTHQUAKES

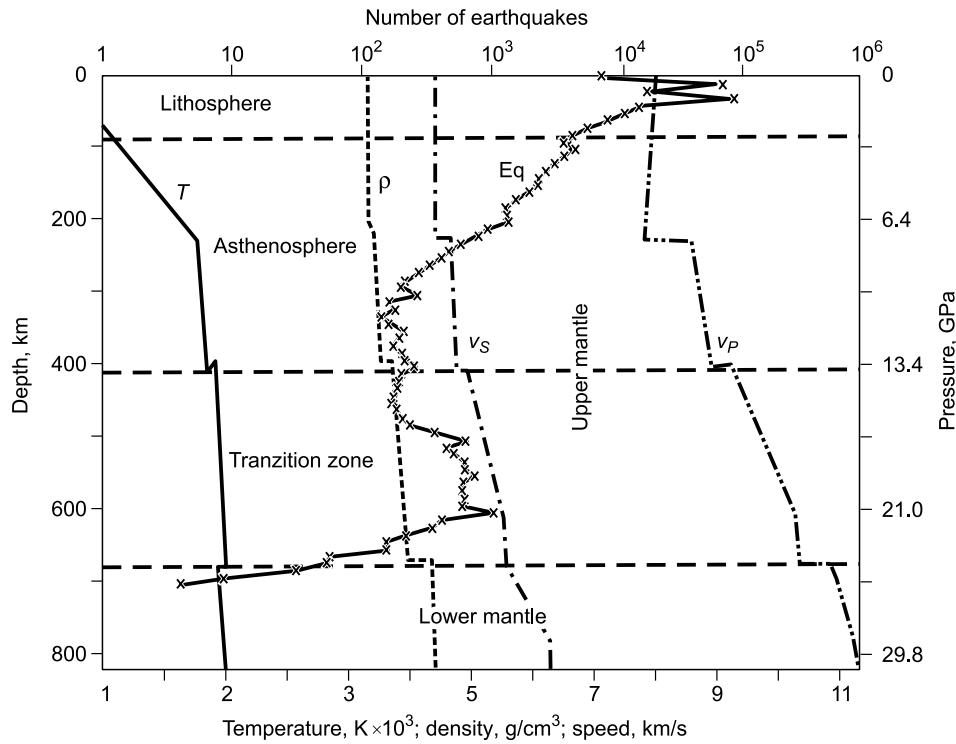
The U.S. Geological Survey database (<https://earthquake.usgs.gov/earthquakes/search>) was used to analyze the spatial distribution of deep-focus earthquakes. Here, a 117-year (1900.07.29–2017.10.27) set of seismic events with  $M \geq 4.5$  were statistically analyzed. The seismic network that existed in the Far East in the last century did not allow precise definition of an earthquake location (epicenter coordinates and hypocenter depth) of earthquakes with  $M < 4.5$  (Levin et al., 2008); therefore, those seismic events were not taken into account. The initial set of seismic events included 234,310 earthquakes that had occurred all over the world.

Figure 1 shows the distribution of earthquakes across the globe relative to the depth of their hypocenters located along the convergent plate boundaries; there is a gradual increase in the hypocenters depths from deep-seated trenches towards the continent (overriding plate). In our case it is the boundary between the Pacific and Amurian (Japan island arc), the Pacific and Okhotsk (Kurile–Kamchatka arc)

plates. This figure shows the significant difference in the distance between the subduction front (epicenters of shallow seismic events) and epicenters of deep focus earthquakes located in the west, far from deep trenches (1600 km for the Japan arc; 750 km for the Kurile–Kamchatka arc; Fig. 1).

For all 234,310 earthquakes we studied the distribution of seismic events as a function of depth using 10-km interval. The plot (Fig. 3) clearly demonstrates a bimodal distribution of earthquake frequency in the upper 50 km, where they amount to over 69% of all recorded seismic events. The plot shows a monotonous decrease in rate of occurrence of earthquakes between 50 and 300 km and a steady earthquake frequency to the depth of 450 km (about 200 events each 10 km) with a small local maximum (259 events) at the depth of 405 km, which is interpreted as the boundary of the first phase transition in the upper mantle (Fig. 3). In the transition zone from about 465 km the frequency of earthquakes per each 10 km markedly increases, thus reaching its maximum at the depth of 605 km (1003 events); then the rate of earthquake occurrence decreases to zero at the upper- and lower-mantle interface (Fig. 3). The deepest earthquake was recorded on May 6, 2007 in the subduction wedge of the Kermadec–Tonga island arc ( $701 \pm 31$  km).

Figure 3 shows a separate set of deep-focus earthquakes in the depth interval between 450 and 700 km, whose distribution was analyzed in this study (9504 events in total; Fig. 4, histogram). The first deep focus earthquake was instrumentally detected on January 1, 1919 close to Fiji Islands; then starting from the 1970s frequency of deep-focus earthquakes over a 5 year period (Fig. 4, histogram) becomes constant (about 1000). However, there are some significant variations in the rate of deep-focus earthquake occurrence: only 394 deep-focus seismic events were recorded for 2014. All earthquakes from this set are related to subduction processes (Fig. 4, Table 1). The lowest rate of deep-focus earthquake occurrence (13) is found for the Eurasian–



**Fig. 3.** Distribution of earthquake hypocenters (Eq), temperature ( $T$ ), density ( $\rho$ ), velocities of ( $V_p$ ) and transverse (secondary) ( $V_s$ ) seismic waves with depth. Hypocenter of earthquakes ( $M \geq 4.5$ ) through the globe. Catalog of earthquakes, US Geological Survey (<https://earthquake.usgs.gov/earthquakes/search/>), 1900.07.29–2017.10.27 (<https://earthquake.usgs.gov/earthquakes/search/>). PREM characteristics ( $T$ ,  $V_s$ ) are given from (Kaminsky, 2017).

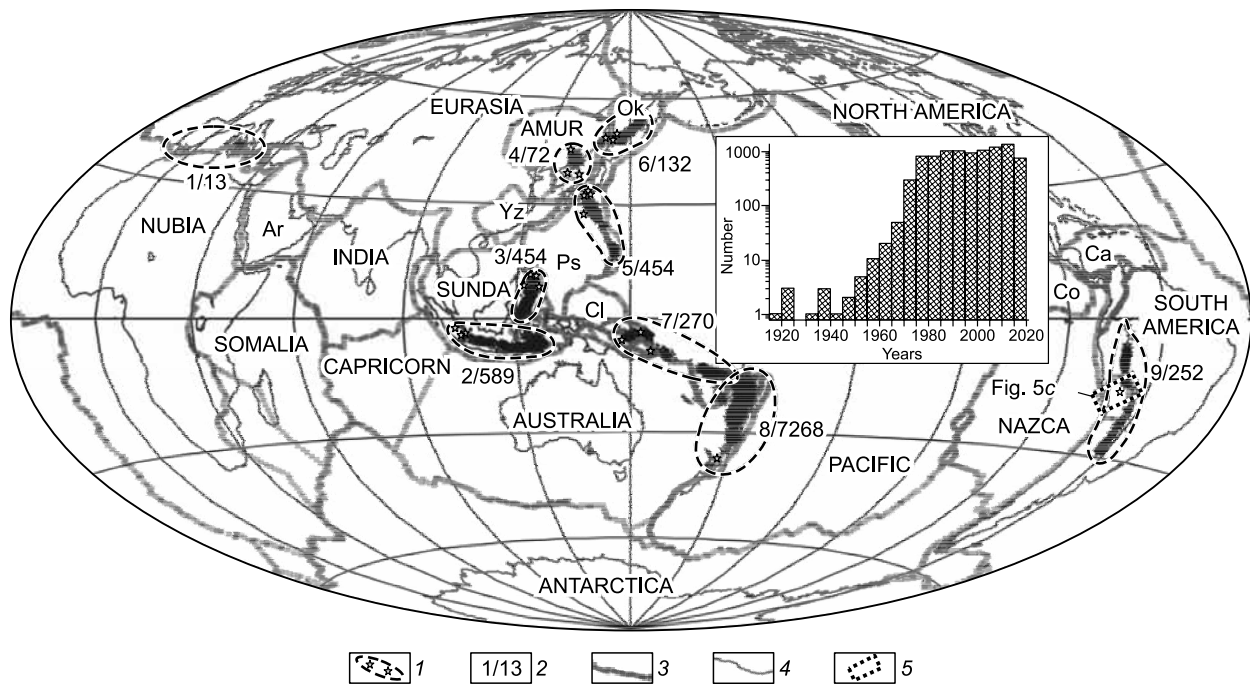
Nubian plate in the area of Gibraltar and Calabrian paleoarcs. The largest number of earthquakes (7268 or over 76% of the 9504 events under analysis) was detected for the recent Tonga–Kermadec island arc. It might be more likely explained by the highest rate of convergence of the Pacific plate beneath the Australian one (Bevis et al., 1995). As shown by the spatial distribution of the selected earthquakes (Fig. 4,

Table 1) one and the same plates could be subducting and overriding: the northern margin of the Australian plate is subducting beneath the Sunda plate (Sunda island arc) and the Pacific plate (Solomon and New Hebrides island arcs) and the eastern part of the Australian plate is overriding the Pacific plate along the Tonga–Kermadec island arc. Another example is the Philippines island arc: its southwest margin

**Table 1.** Characteristics of zones with earthquakes with hypocenter depths between 450 and 700 km

No.	Island arc/marginal volcanic belt	Subducting plate	Overriding plate	Number of earthquakes	Maximum magnitude	Maximum depth, km	$b$	$r_k$
1	Gibraltar and Calabrian	Nubian (African)	Eurasian	13	7.8	626	–	–
2	Sunda	Australian	Sunda	589	7.9	676	–0.779 ± 0.061	–0.985
3	Philippine	Philippine	Sunda	454	7.6	678	–0.710 ± 0.078	–0.971
4	Japan	Pacific	Amirian	72	7.3	608	–0.348 ± 0.064	–0.938
5	Mariana	Pacific	Philippine and Mariana	454	7.8	683	–0.709 ± 0.067	–0.979
6	Kurile–Kamchatka	Pacific	Okhotsk	132	8.3	679	–0.480 ± 0.035	–0.984
7	Solomon and New Hebrides	Australian	Pacific	270	7.3	700	–0.871 ± 0.068	–0.988
8	Tonga–Kermadec	Pacific	Australian	7268	7.8	701	–0.999 ± 0.029	–0.998
9	Andean	Nazca	South American	252	8.2	650	–0.420 ± 0.045	–0.967
	Total	–	–	9504	8.3	701	–0.880 ± 0.043	–0.993

Note.  $b$ , coefficient of inclination of earthquake frequency plot,  $r_k$ , coefficient of Spirmen correlation. The number in the corresponds to the area number in Fig. 4.



**Fig. 4.** Geographic location of earthquake ( $M \geq 4.5$ ) epicenters with depths of  $\geq 450$  km, histogram of annual earthquake frequency. Molweide projection, central meridian of  $150^\circ$  E. 1, areas of deep-focus earthquakes; 2, zone number (numerator) and number of earthquakes (denominator), correspond to the data of Table 1; 3, plate boundaries (Argus et al., 2011); 4, coastline; 5, band synthesized profiles of earthquake hypocenter depths shown in Fig. 5.

is subducting beneath the Sunda plate (Philippines island arc), while its northeast part is overriding the Pacific plate (Mariana island arc). Over 83% of deep-focus earthquakes are related to the subduction of the Pacific plate (Fig. 4).

For most of the earthquakes the magnitude was calculated from the amplitudes of the body waves (8107 of 9504 selected earthquakes); for very large earthquakes we calculated the moment magnitude using different methods. As it is hard to compare the relative amounts of energy released during earthquakes as the energy scales are different, the plot of deep-focus earthquake frequency has not been compiled.

To analyze the spatial distribution of earthquakes throughout the Japan and Kurile–Kamchatka island arcs as a function of depth we constructed two synthesized profiles crossing their structures perpendicular to their strikes (Figs. 1, 5). The major differences in the structures of those arcs include: (1) subducted slabs<sup>1</sup> projected onto the surface appear to be almost 2 times different in size:  $\sim 1500$  km for the Japan arc (Fig. 5a) and  $\sim 600$  km for the Kurile–Kamchatka arc (Fig. 5b); therefore the slab subduction angle is different: the dip of the subducting Pacific plate changes from  $30^\circ$  beneath the Amurian plate to about  $45^\circ$  beneath the Okhotsk plate; (2) It is generally assumed that the maximum hypocenter depth of earthquakes within the slab beneath the Japan arc is about 600 km (Fig. 5a), all of those earthquakes occurred in the transitional zone markedly

higher than the phase transition discontinuity at the upper- and lower-mantle boundary (Fig. 3). Regarding the Kurile–Kamchatka arc, deep-focus earthquakes (660 km) appear to penetrate the phase-transition discontinuity at the upper- and lower-mantle boundary (Fig. 5b). Then, the lower slab boundary flattens to the west for over 150 km.

The situation is the same for the Peru–Chile subduction zone with the second largest deep-focus earthquake ever recorded (Kikuchi and Kanamori, 1994; Zhan et al., 2014): (1) the subducted slab projected onto the surface is about 750 km and the Pacific Plate is subducting beneath the South American plate at an angle of approximately  $40^\circ$ ; (2) the largest deep-focus earthquake (09.06.1994) and its largest aftershock (08.08.1994) took place close the upper–lower mantle boundary (Figs. 4, 5c).

#### GREATEST DEEP-FOCUS EARTHQUAKES IN SUBDUCTION ZONES: CHARACTERISTICS OF FOCAL MECHANISMS

It has been found that the structure of subducting slabs beneath the Kurile–Kamchatka and Japan island arc systems are different. Therefore, the focal mechanisms of the large earthquakes, occurring here, are different.

First we discuss possible focal mechanism solutions (here and after we use Harvard CMT Catalog <http://www.globalcmt.org/CMTsearch.html>) for the two largest deep-focus earthquakes ( $M_w = 7.3$ ), recorded in the active slab beneath the Japan island arc (Fig. 5a). The first July 21,

<sup>1</sup> Slab description is given from the location of earthquake hypocenters in the subduction zone.

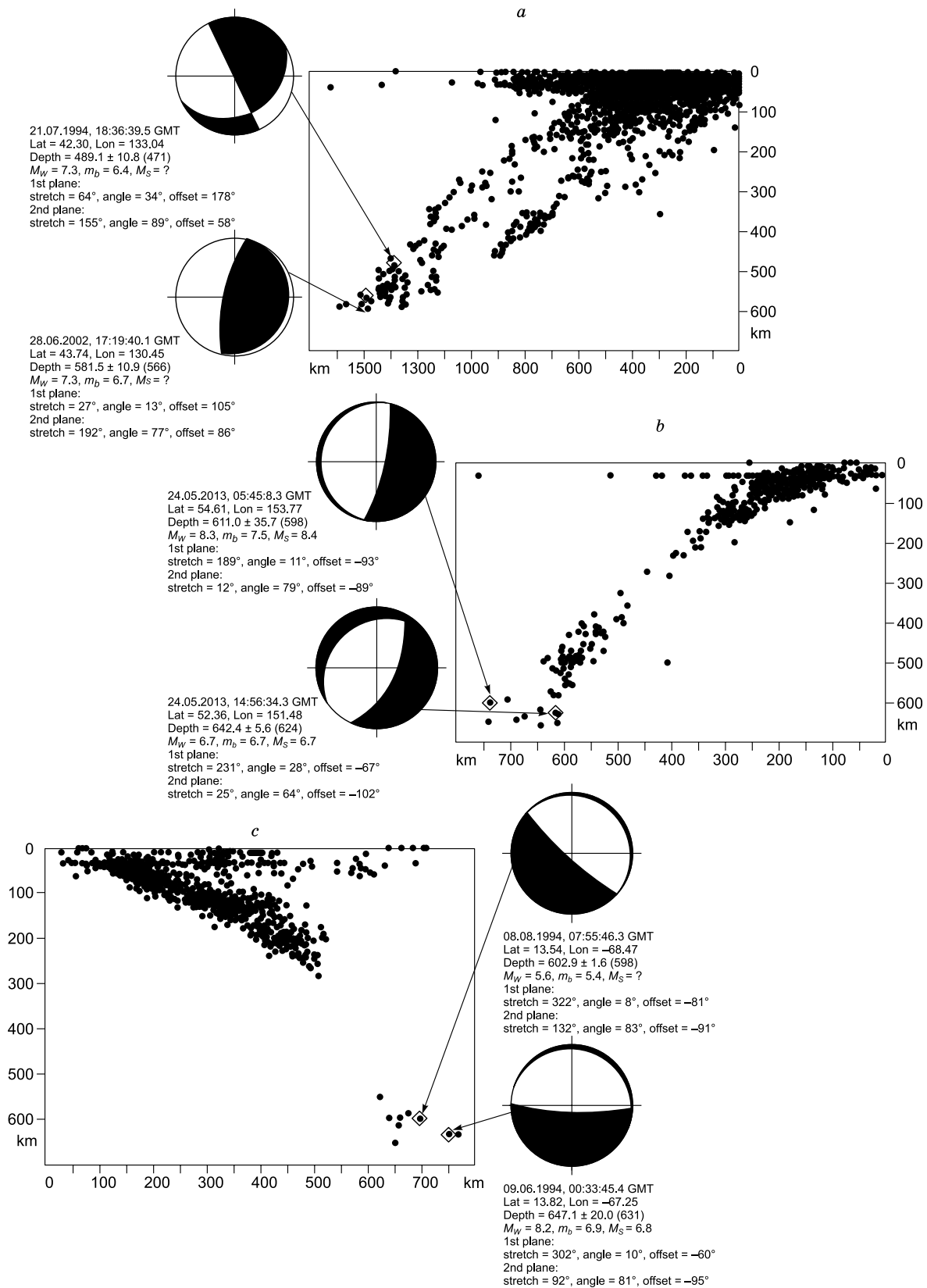


**Fig. 5.** Distribution of earthquakes on synthesized depth profiles for the Japanese (a) and Kurile–Kamchatka (b) island arcs, Peru–Chile marginal volcanic belt (c). Focal mechanisms are from GCMT (<http://www.globalcmt.org/CMTsearch.html>), calculated by (Dziewonski et al., 1981; Ekström et al., 2012). Hypocenter depths based on data by U.S. Geological Survey (<https://earthquake.usgs.gov/earthquakes/search>) are given in round brackets.

1994 seismic event took place at the depth of 489 km<sup>2</sup> with the epicenter located in the Sea of Japan at about 50 km south of Nakhodka city as a response to the buildup of mainly compressive stresses on a reverse fault with a small strike-slip component. One of the possible rupture plane solutions indicates an overall strike of 64° and the dip angle of 34°, while the second one shows an overall strike of 155° and dip angle of 89° (Fig. 5a). The second event, June 28, 2002 earthquake, was produced at the depth of 592 km with the epicenter located 100 km west of Ussuriisk city, from the buildup of mainly compression stresses on a reverse fault. One of possible rupture plane solutions indicate its overall strike of 27° and the dip angle of 13°, while the second one shows the strike of 192° and dip angle of 77° (Fig. 5a). Both earthquakes occurred in the inclined (active) part of the slab in the transition zone markedly higher than the upper- and lower mantle boundary.

The situation is different in case of the largest ( $M_w = 8.3$ ) deep-focus earthquake occurring on 24 May 2013 beneath the Kurile–Kamchatka arc and its aftershock ( $M_w = 6.7$ ). The Okhotsk mainshock took place at a depth of 611 km with the epicenter located in the Sea of Okhotsk 150–160 km west off the Kamchatka Peninsula as a response to the buildup of mainly tension stresses on a normal fault. One of the possible rupture plane solutions has an overall strike of 189° and the dip angle is 11°, while the second one shows a strike of 12° and a dip angle of 79° (Fig. 5b). About 9 hours later, the second event (aftershock) occurred at a depth of 642 km with the epicenter located 318 km southwest of the mainshock as result of buildup of tension stresses on normal fault with a negligible right-lateral shear component. One of possible rupture plane solutions indicate its overall strike of 231° and the dip angle of 28°, while the second one shows a strike of 25° and a dip angle of 64° (Fig. 5b). Both earthquakes occurred at a depth close to the upper-lower mantle interface. A great number of aftershocks recorded by the Kamchatka Branch of the Geophysical Survey, RAS should be noted: 12 of them had a magnitude ( $M \geq 4$ ) and hypocenters depths ranging between 500 and 640 km (Chebrov et al., 2015; Varga et al., 2017).

Another large deep earthquake, similar in magnitude and focal mechanism, took place on June 6, 1994 on the opposite coast of the Pacific Ocean beneath the Peru–Chile subduction zone (Fig. 4). The mainshock ( $M_w = 8.2$ ) occurred at a depth of 647 km with the epicenter located 300 km north off La-Pas city (Bolivia) and was a result of tension stresses buildup on a normal fault (Kikuchi and Kanamori, 1994; Zhan et al., 2014). The fault plane solutions indicate the strike directions for two possible planes as 302° and 92° and dip angles of 10° and 81°, respectively (Fig. 5c). About two months later, the largest aftershock ( $M_w = 5.6$ ) occurred ~90 km to the west of the mainshock at a depth of 603 km

as a result of normal fault dislocation. The fault plane solutions fix the strike directions for two possible planes as 322° and 132° and dip angles of 8° and 83°, respectively (Fig. 5c). Like in case with the earthquake beneath the Kurile–Kamchatka arc, both events (mainshock and aftershock) beneath the Peru–Chile subduction zone took place around the upper-lower mantle boundary (Fig. 5c).

The analysis of spatial location for these two large deep earthquake and the generalization of their focal mechanism solutions suggest that all those seismic events occurred close to the upper–lower mantle boundary and were a response to buildup of mainly tension stresses. As follows from Fig. 3 in (Varga et al., 2017) extensional stresses dominate in most of the deep earthquakes with a moment magnitude ( $M_w$ )  $\geq 7.0$  happening in the time span between 1976 and 2010 (Harvard CMT Catalog).

Two questions may arise. Firstly, why in some subduction zones (e.g., Kurile–Kamchatka and Peru–Chile) earthquakes occur almost around the upper–lower mantle boundary, while in others (e.g., Japan island arc system) they take place at shallower depth markedly higher than the upper-lower mantle interface (Fig. 5a). It seems to us that this difference can be only explained by the dip angle of the active slab segment that determines the structure of the slab’s bottom. The seismic tomography shows (Van der Hilst et al., 1993; Li et al., 2008) that in case of “steep” subduction with a dip angle of 40°–45° (Fig. 5b, c) the active lower slab part crosses the upper-lower mantle interface, while the stagnant slab segment is not so prominent (tomography profiles Nos. 11, 12 for the Kurile–Kamchatka arc (Fig. 10 from (Li et al., 2008)) and tomography profiles Nos. 7, 8, 9 for Peru–Chile subduction zone (Fig. 9 from (Li et al., 2008))). Similar interpretation was given for the Kurile–Kamchatka arc in (Koulakov et al., 2011): 13 vertical sections across the strike of the arc were obtained using the *P*- and *S*-velocity anomalies. Close to the location of the 2013 Okhotsk Sea earthquake (sections 8, 9, 10, 11 on Fig. 4 in (Koulakov et al., 2011)) the active slab boundary penetrates the phase transition discontinuity around the upper-lower mantle interface and is traced down to 800 km.

Secondly, why those large deep earthquakes occur at the bottom of the lower mantle in the extensional stress environment (Fig. 5b, c). If we take a “standard” model for the morphology of the slab lower boundary (steep slab geometry (active slab) → bending → almost horizontal stagnant section of the slab), then tectonic twisting and tectonic compression should take place. However, these two largest deep earthquakes and their aftershocks are related to normal faults, occurring around the upper-lower mantle boundary.

In case of “flat” subduction with a convergence angle of  $<30^\circ$  (Fig. 5a), the active segment of the slab “enters” the upper-lower mantle boundary and then sinks to a depth where the slab begins flattening near horizontally to apparently stagnate over thousands kilometers beneath the Eurasian continent (tomography profiles 13, 14 for the Japan island arc (Fig. 10 from (Li et al., 2008))). However, in the

<sup>2</sup> Note a systematic difference in the depth of earthquake hypocenters in database U.S. Geological Survey (<https://earthquake.usgs.gov/earthquakes/search/>) и GCMT (<http://www.globalcmt.org/CMTsearch.html>) for about 15 km (Fig. 4).



stagnant slab segment a gradual increase in temperature and viscosity makes the occurrence of a large earthquake unlikely. The model (Zhao and Tian, 2013; Chen et al., 2017) indicates that the within-plate volcanoes in continental China (Changbai and Wudalianchi) are related to upwelling flows of the hot and humid asthenospheric material above the stagnant slab segment beneath the Japan island arc.

#### TRANSITION BETWEEN LINEAR AND BENT FORMS OF $\text{SiO}_2$ AND ITS POSSIBLE INFLUENCE ON THE INITIATION OF EARTHQUAKES AT THE UPPER–LOWER MANTLE BOUNDARY

Twenty six deep-focus ( $>400$  km) large ( $M_w > 7$ ) earthquakes that occurred from 1994 to 2013 were studied by applying a multiple source inversion method based on waveform modeling (Chen and Wen, 2015). All the events were classified into three categories (Chen and Wen, 2015). We focus only on one group, represented by the Bolivia and Okhotsk earthquakes. Chen and Wen (2015) suggested that the initial processes of these large deep-focus earthquakes can be best explained by a cascading failure of shear thermal instabilities in weak shear zones subjected to stress accumulation. The focal mechanisms of these two largest ever-recorded deep earthquakes (Bolivia and Okhotsk) and their large aftershocks are similar: all of them were generated by normal faults within stagnant slabs. Moreover, fault plane solutions show planes that trend approximately parallel to subduction zones (Figs. 4, 5b, c). The similarity in the physical mechanisms to generate these two earthquakes as well as the similarity in their waveforms suggests that these seismic events can be grouped together into one category and thus the model of a cascade earthquake related to shear instability can be proposed (Chen and Wen, 2015).

Another mechanism proposed for deep earthquakes (particularly the Okhotsk event) is related to the destruction of mantle minerals including metastable olivine transforming into spinel in a cold subducting slab (Kirby et al., 1991; Ye et al., 2013; Lyskova, 2014). An increase in the shear stresses could trigger the phase transition, which is primarily confined to the fault plane. Moreover, sharp changes in the crystalline structure could initiate frictional sliding even under high hydrostatic pressures at those depths. This is true for rocks within a cold slab subducting into the deep mantle: the depth of phase transitions within the subducted slab depends on the composition, temperature and subducting rate and could correspond to the lower boundary of the mantle transition zone (Kirby et al., 1991; Lyskova, 2014). As a result, the earthquakes are generated. The increase in sliding velocities resulting in the frictional heat could lead to melting of the rupture surface thus causing further propagating of the rupture front (Kanamori et al., 1998; Ye et al., 2013).

The mechanism that initiates deep earthquakes occurring within the subducting slab in the upper–lower mantle transition zone (Fig. 6) is a polymorphous olivine to spinel phase

change (Kirby, 1987; Kirby et al., 1996). This phase transition suggests variations in the crystalline structure and rock hardness thus provoking the reverse faulting earthquakes.

Recent studies (Khleborpos et al., 2016, 2017) provide grounds for the hypothesis put forward earlier stating that in mantle minerals the  $\text{SiO}_2$  molecule could undergo a transition from the linear structure to bent form. It mainly concerns relatively independent  $\text{SiO}_2$  “quasimolecules”. In mantle melts,  $\text{SiO}_2$  fragments are thought to form certain clusters; the difference of the corresponding forces gives reason to apply an approximation of relatively independent  $\text{SiO}_2$  “quasimolecules”. The stishovite crystalline structure (silicon coordination number is 6) is characterized by  $\text{O}=\text{Si}=\text{O}$  linear groups; each of them is connected to four other such groups via  $\text{Si}\dots\text{O}$  coordination type bonds (Gabuda and Kozlova, 2009). We can assume that such linear  $\text{O}=\text{Si}=\text{O}$  groups could exist in mantle melts, however, they could be bound to such other groups by weaker  $\text{Si}-\text{O}$  bonded interaction. It could be suggested further that the difference in the strength of those bonds is so great that  $\text{O}=\text{Si}=\text{O}$  fragments in the melts could be regarded as relatively independent and these  $\text{O}=\text{Si}=\text{O}$  fragments are considered in the first approximation as free molecules undergoing the transition to the bent form. As mentioned above, the energy released from the transition from bent  $\text{SiO}_2$  structure to linear  $\text{SiO}_2$  structure is relatively high (about 2.5 eV or 4000 kJ/kg). According to calculations (Gabuda and Kozlova, 2009) a  $\text{SiO}_2$  molecule could undergo a transition from the linear structure to the isomeric cyclic (bent) form at higher pressures like those occurring in the mantle transition zone. In the first approximation the pressure required for the transition from linear to bent form can be estimated as  $P \sim A/\Delta V$  where  $A$  corresponds to a height of potential barrier between the considered states,  $\Delta V$  is the difference of volumes between bent and linear structures of the  $\text{SiO}_2$  molecule. Using the calculations of geometry parameters of the bent  $\text{SiO}_2$  form,  $\Delta V$  can be estimated as  $15.4 \times 10^{-30} \text{ m}^3$ . Assuming  $A \sim 2$  eV, then  $P \sim 22$  GPa.

This hypothesis needs further checking calculations. Those calculations, however, are rather complicated. On the other hand, exact quantitative results that exclude this hypothetical transition of  $\text{SiO}_2$  molecule, are unknown. Therefore, this study presents only the qualitative data given above and admits the existence of relatively independent  $\text{O}=\text{Si}=\text{O}$  fragments in melts of mantle minerals at higher pressures.

Around the upper–lower mantle boundary a slab strongly deforms thus resulting in further pressure increase. The phase transition at this depth (Fig. 3) however, inhibits the subducting slab to sink, thus causing deformation of its lower edge and a corresponding growth of mechanical stresses (Lyskova, 2014). Stress energy is released, thus leading to earthquakes.

As noted above, in the focus of deep earthquakes the friction due to intensive sliding could induce shear melting close to the rupture surface (Kanamori et al., 1998; Ye et al., 2013; Lyskova, 2014). It is also known that shear melting

through the effect of temperature increase and sliding could lead to partial melting of rock (Karato et al., 2001; Lyskova, 2014).

It can be assumed that in the mantle transition zone the  $\text{SiO}_2$  bent structure could form close to the rupture surface at the corresponding pressures. Moreover, a feedback system, ( $\text{SiO}_2$  transition-melting/sliding), could occur. When the mantle substance is destroyed in some regions, the mechanical stresses then drop sharply and therefore the energy from the transition of a  $\text{SiO}_2$  fragment from bent to linear structure is released. If the energy from this transition (“explosion”) is sufficient for the propagation of rupture into adjacent regions of the mantle substance, the net of the corresponding “explosion roads” should appear. Therefore, the volume of substance and energy, involved into these processes, would appear to be large enough to initiate an earthquake with the energy several orders higher than the energy of simple mantle phase transitions of linear  $\text{SiO}_2$ -form molecules. This mechanism could contribute to the generation of deep-focus earthquakes with huge energy. Note, that this mechanism could be plausible both for the thermal shear instability model and for the scenario where the metastable olivine transforms into spinel in a cold subducting slab.

Our model (Fig. 6) with large deep earthquakes show that they occur around the upper–lower mantle boundary during the slab bending. As the slab bends, heat and fluids tend to rise from the lower mantle (Zhao and Tian, 2013). This heat

and mass flux takes place in pulses due to the shielding effect of the cold material within the stagnant slab. As a result, heat and fluids are the cause of the reverse transition of the bent form of  $\text{SiO}_2$  fragments to a linear structure leading to an additional release of heat and a subsequent shear melting of rocks due to heat accumulation in the zone of shear stresses provoking a combined avalanche-like increase of temperature and strain rate similar to that observed in “shear instability” model (Ogawa, 1987). Thus, deep-focus earthquake with a normal fault component can be generated. Another cause initiating large earthquakes within the upper mantle transition zone is an increase in slab’s thickness (Koulakov et al., 2011) that causes the subduction to slow down and the matter to accumulate in the transition zone between the 410 km and 670 km discontinuities. When the critical mass is reached over the 670 km boundary, the drop-like body begins to submerge into the denser and more viscous lower mantle as is observed from the seismic tomograms of the arc center. Separation of a “drop” from the slab is accompanied by normal faulting (Fig. 6).

## CONCLUSIONS

The modern Earth’s endogenous activity is determined by deep geodynamics, which is characterized by a combination of plate tectonics and plume tectonics. The subduction process became one of the most important factors to initiate plate tectonics at about 3 Ga and to bring it to operation at about 2 Ga. Another important factor of plate tectonics is the seafloor spreading process, which also affects the Earth’s surface. These two important features of plate tectonics, i.e., subduction and spreading are responsible for building many of the features we see on the Earth’s surface today as well as for its interior in particular for the interaction of the Earth’s inner layers. So, it is important to study the mechanisms that can explain how subduction is linked to deep-focus earthquakes and the origin of active continental margins, which host many mineral deposits. The answer to this question requires the efforts of many specialists (geologists, chemists, physicists). As explained above, subduction generally occurs in active tectonic zones characterized by frequent earthquakes and volcanic activity. Such zones may include island arcs, active continental margins or collage of continental blocks (like the Caucasus) or continental to continental plate collision (India–Eurasia continental collision). This study focuses on Kurile–Kamchatka and Japan arc systems, where the Pacific lithospheric plate sinks back into the mantle. The plate submerges to the upper–lower mantle boundary located at a depth of 670 km, which is attributed to changes in temperature and density (Maruyama, 1994; Condie, 2011). The subducting slab sinks to this boundary and then seems to stagnate as the slab thickens due to the added lithospheric material thus forming a megalith (Maruyama, 1994) that is traced down to 800 km beyond the phase transition boundary. As shown by seismic tomography (Condie, 2011; Do-

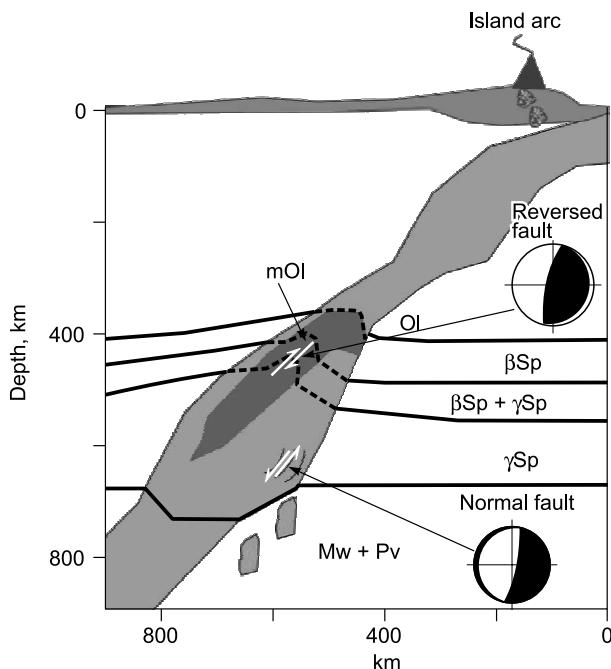


**Fig. 6.** Scheme of the subducting slab of the oceanic lithosphere and deep-focus earthquakes in the upper mantle transition zone with elements of mantle mineralogy. The thermal model of the subducting slab (Kirby et al., 1996) and seismic tomography data for the Kurile–Kamchatka arc (section 10, Fig. 4 from (Koulakov et al., 2011)) are used. Ol, olivine phase, mOl, phase of metastable olivine,  $\beta\text{Sp}$ , phase of modified spinel,  $\gamma\text{Sp}$ , spinel phase,  $M_w$ , magnesium wüstite, Pv, perovskite.

bretsov, 2011; Kuzmin et al., 2011), the slab splits and its upper part moves along the boundary with the lower mantle towards the continents, while the second part separated into several blocks, sinks into the lower mantle reaching the D'' layer, located at a core–mantle interface. Such a structure was derived for the subducting slab beneath the Kurile–Kamchatka arc based on seismic tomography results (Koulakov et al., 2011).

Another mechanism is that the lithospheric slab does not sink into the lower mantle but lies down in the mantle transition zone, bends and then moves along the upper–lower mantle boundary towards the continent (Irifune and Ringwood, 1993). As shown by geophysical data (Irifune and Ringwood, 1993) such a mechanism is typical of younger, thin lithosphere with a relatively shallow depression stretching over 1000 km below a slab. In both models, lithospheric slabs are thought to split and sink into the lower mantle (Condie, 2011).

With the seismic data presented here we show that these two models are plausible. Here, we describe processes related to phase transitions as possible factors to initiate deep-focus earthquakes taken into account the first model that predicts lithosphere slab splitting around the upper–lower mantle boundary.

The model illustrating our ideas on processes occurring in the lithosphere megalith that penetrates into the lower mantle over 150 km was compiled using the previous modeling from (Kirby et al., 1996; Koulakov et al., 2011) supplemented by our data on phase transitions. The descend of the lithospheric slab can be described either by phase transitions or shift faulting that initiate deep-focus earthquakes and possibly melting of the subducted material along the fault. As mentioned above the slab penetrates into the mantle with relatively high subduction rate i.e., it remains cold with respect to the ambient mantle. As was demonstrated by paleogeographic reconstructions (Kuzmin et al., 2010, 2011) over most of the Phanerozoic Siberia was drifting within the African hot mantle field or large low shear velocity province (LLSVP). In the Cretaceous the Siberian continent overlapped the eastern margin of the Pacific hot mantle field. Therefore, rocks with island arc chemistry (subduction-related) and those related to plume magmatism occur here (Yarmolyuk et al., 2013).

As is known, the Earth's core is made of two layers: the inner solid core and outer liquid core which is less dense than iron as it contains abundant volatile elements (Litasov and Shatsky, 2014). During the Earth's accretion period at higher temperatures and pressures primordial hydrogen and helium could form stable compounds He–H, He–O, He–Si, He–metals that were stored in the Earth's core (Gilat and Vol, 2012). During the core segregation volatile elements remained in the outer core, hence accounting for its lesser density relative to the inner core. Volatiles would likely lead to the origin of mantle plumes within the D'' layer which are expressed on the surface as hot spots. High relative abundances of primordial helium that are commonly found in

Hawaiian basalts are thought to be derived from mantle plumes. Therefore, mantle-derived hot fluids could reach a depth where the subducted lithosphere forms megaliths. These mantle-derived hot fluids are thought to have an important role in generating earthquakes (Gilat and Vol, 2012). As shown by the scheme (Fig. 6) they contribute to causing the temperature increase of the subducted oceanic lithosphere and therefore phase transitions.

Experiments by Irifune and Ringwood (1993) suggest that the assemblage of majorite + CaSiO<sub>3</sub>-rich perovskite + stishovite could be displayed by the MORB composition at pressures up to 28 GPa, and at 1200 and 1500 °C. The experiments show that at pressures lower than 28 GPa it would be displayed by majorite-garnet assemblage, containing mostly garnetite, hence accounting for the slab buoyancy relative to the ambient mantle. The underlying layer of harzburgite within the slab is displayed by magnesium wüstite + perovskite assemblage that would be 0.05 g/cm<sup>3</sup> less dense than the lower mantle (Irifune and Ringwood, 1993) thus causing an unstable equilibrium in buoyancy relationships between the subducting slab and lower mantle. This unstable equilibrium could be broken by a transition of SiO<sub>2</sub> quasimolecules from the bent form to the linear structure. However, this supposition needs refining using mathematical modeling.

The hypothesis of such a transition is the following. As shown by quantum chemical calculations the SiO<sub>2</sub> molecule tends to transform from linear to isomeric bent form or vice versa and the energy released from the transition can amount to about 240 kJ/mole (Gabuda and Kozlova, 2009). The hypothetical crystal structure with SiO<sub>2</sub> bent form could be similar to the paratellurite (β-TeO<sub>2</sub>) structure in the tetragonal syngony, but the existence of liquid silica, consisting of angular SiO<sub>2</sub> molecules is also possible. The studies (Khleborpos et al., 2016, 2017) provide grounds for the hypothesis stating that in mantle minerals SiO<sub>2</sub> quasimolecules could undergo a transition to bent (cyclic) form. According to estimates (Gabuda and Kozlova, 2009) the SiO<sub>2</sub> molecule undergoes such a transition from the linear to bent form under higher pressures like those existing in the mantle transition zone. On the other hand, around the upper–lower mantle boundary a slab strongly deforms thus resulting in further pressure increase. Taking into account that shear melting could be induced close to the rupture surface, it can be suggested that: (1) a layer of SiO<sub>2</sub> fragments with cyclic structure can be formed close to the rupture surface; (2) when the mantle substance is destroyed in some region, the mechanical stresses then drops sharply and therefore the energy from the transition of SiO<sub>2</sub> fragments from bent to linear structure is released. If the energy of this transition (“explosion”) is sufficient for the propagation of rupture into adjacent regions of the mantle substance, a feedback system (SiO<sub>2</sub> transition-melting/sliding), triggering the deep earthquakes, could emerge; (3) this mechanism is plausible to describe splitting of the subducting oceanic plate.

Thus, the proposed hypothesis describes the mechanism of large deep-focus earthquakes taking into account the seismic tomography data demonstrating a splitting of the subducting slab: its upper part (involving oceanic crust and sediments) moves “horizontally” towards the continent, while its lower part separated into blocks subsides into the lower mantle. We must note that the recycling of the upper slab part could be a source for igneous rocks in the Primorye and Eastern Asia. The criteria to distinguish between the plume-related within-plate rocks and those originated as result of the older crust recycling have to be deduced during further studies.

In conclusion we note that the problem discussed here was first posed by Rem G. Khlebopros who will be remembered by future generations of researchers in different fields (geology, chemistry, physics).

The authors are grateful to Yu.A. Morozov, A.R. Oganov, V.A. Slepikov and V.V. Yarmolyuk for fruitful discussion and valuable remarks.

The study was accomplished in terms of the State Project IX.130.3.1—No. 0350-2016-0032 and was supported by the Russian Science Foundation (grant No. 16-17-00015), the Russian Foundation for Basic Research (grant No. 17-05-00928), and Siberian Federal University (project P218).

## REFERENCES

- Argus, D.F., Gordon, R.G., DeMets, C., 2011. Geologically current motion of 56 plates relative to the no-net-rotation reference frame. *Geochem. Geophys. Geosyst.* 12 (11), Q111001. DOI:10.1029/2011GC003751.
- Belov, N.V., Godovikov, A.A., Bakakin, V.V., 1982. *Outlines of Theoretical Mineralogy* [in Russian]. Moscow, Nauka.
- Bevis, M., Taylor, F.W., Schutz, B.E., Reay, J., Isacks, B.L., Helu, S., Singh, R., Kendrick, E., Stowell, J., Taylor, B., Calmant, S., 1995. Geodetic observations of very rapid convergence and back-arc extension at the Tonga arc. *Nature* 374 (3), 249–251.
- Chebrov, V.N., Kugaenko, Yu.A., Vikulina, S.A., Kravchenko, N.M., Matveenko, E.A., Mityushkina, S.V., Raevskaya, A.A., Salykov, V.A., Chebrov, D.V., Lander, A.V., 2013. The deep earthquake in the Okhotsk Sea of May 24, 2013 with magnitude  $M_w = 8.3$ —the strongest seismic event off the Kamchatka coast during the period of the detailed seismological observations. *Vestnik KRAUNTS, Nauki o Zemle* 21 (1), 17–24.
- Chebrov, A., Yu., Chebrov, V.N., Gusev, A.A., Lander, A.V., Guseva, E.M., Mityushkina, S.V., Raevskaya, A.A., 2015. The impacts of the  $M_w$  8.3 Sea of Okhotsk earthquake of May 24, 2013 in Kamchatka and worldwide. *J. Volcanol. Seismol.* 9 (4), 223–241.
- Chen, H., Xia, Q.-K., Ingrin, J., Deloule, E., Bi, Y., 2017. Heterogeneous source components of intraplate basalts from NE China induced by the ongoing Pacific slab subduction. *Earth Planet. Sci. Lett.* 459, 208–220.
- Chen, Yu., Wen, L., 2015. Global large deep-focus earthquakes: Source process and cascading failure of shear instability as a unified physical mechanism. *Earth Planet. Sci. Lett.* 423, 134–144.
- Condie, K.C., 2011. *Earth as an Evolving Planetary System*. Elsevier.
- Dobretsov, N.L., 2011. *Fundamentals of Tectonics and Geodynamics* [in Russian]. Novosibirsk. Gos. Univ., Novosibirsk.
- Dubrovinsky, L.S., Saxena, S.K., Lazor, P., Ahuja, R., Eriksson, O., Will, J.M., Johansson, B., 1997. Experimental and theoretical identification of a new high-pressure phase of silica. *Nature* 388, 362–365.
- Dziewonski, A.M., Hales, A.L., Lapwood, E.R., 1975. Parametrically simple Earth models consistent with geophysical data. *Phys. Earth Planet. Inter.* 10, 12–48.
- Dziewonski, A.M., Chou, T.-A., Woodhouse, J.H., 1981. Determination of earthquake source parameters from waveform data for studies of global and regional seismicity. *J. Geophys. Res.* 86, 2825–2852.
- Ekström, G., Nettles, M., Dziewonski, A.M., 2012. The global CMT project 2004–2010: Centroid-moment tensors for 13,017 earthquakes. *Phys. Earth Planet. Inter.* 200–201, 1–9.
- Frohlich, C., 2006. *Deep Earthquakes*. Cambridge Univ. Press, Cambridge, U.K.
- Gabuda, S.P., Kozlova, S.G., 2009. *Lone Pairs and Chemical Bonding in Molecular and Ionic Crystals* [in Russian]. Izd. SO RAN, Novosibirsk.
- Gilat, A., Vol, A., 2012. Degassing of primordial hydrogen and helium as the major energy source for internal terrestrial processes. *Geosci. Front.*, 1–11. DOI:10.1016/j.gsf.2012.03.009.
- Irfune, T., Ringwood, A.E., 1993. Phase transformations in subducted oceanic crust and buoyancy relationships at depths of 600–800 km in the mantle. *Earth Planet. Sci. Lett.* 117 (1–2), 101–110.
- Kaminsky, F.V., 2017. *The Earth's Lower Mantle Composition and Structure*. <http://www.springer.com/978-3-319-55683-3>.
- Kanamori, H., Anderson, D.L., Heaton, T.H., 1998. Frictional melting during the rupture of the 1994 Bolivian earthquake. *Science* 279, 839–842.
- Karato, S., Riedel, M.R., Yuen, D.A., 2001. Rheological structure and deformation of subducted slabs in the mantle transition zone: implications for mantle circulation and deep earthquakes. *Phys. Earth Planet. Inter.* 127, 83–108.
- Khlebopros, R.G., Zakhvataev, V.E., Slepikov V.A., Kuzmin, M.I., 2016. On the possibility of phase transitions with the formation of SiO<sub>2</sub> peroxide forms in the earth mantle and their effect on mantle convection. *J. Struct. Chem.* (2), 430–434.
- Khlebopros, R.G., Zakhvataev, V.E., Gabuda, S.P., Kozlova, S.G., Slepikov, V.A., 2017. Possible mantle phase transitions by the formation of SiO<sub>2</sub> peroxides: Implications for mantle convection. *Dokl. Earth Sci.* 473 (2), 416–418.
- Kikuchi, M., Kanamori, H., 1994. The mechanism of the deep Bolivia earthquake of June 9, 1994. *Geophys. Res. Lett.* 21 (22), 2341–2344.
- Kingma, K.J., Cohen, R.E., Hemley, R.J., Mao, H.-K., 1995. Transformation of stishovite to a denser phase at lower-mantle pressures. *Nature* 374, 243–245.
- Kirby, S.H., 1987. Localized polymorphic phase-transformation in high-pressure faults and applications to the physical-mechanism of deep earthquakes. *J. Geophys. Res. B, Solid Earth Planets* 92, 13,789–13,800.
- Kirby, S.H., Durham, W.B., Stein, L.A., 1991. Mantle phase changes and deep earthquake faulting in subducting lithosphere. *Science* 252, 216–225.
- Kirby, S.H., Stein, S., Okal, E.A., Rubie, D.C., 1996. Metastable mantle phase transformations and deep earthquakes in subducting oceanic lithosphere. *Rev. Geophys.* 34, 261–306.
- Koulakov, I.Yu., Dobretsov, N.L., Bushenkova, N.A., Yakovlev, A.V., 2011. Slab shape in subduction zones beneath the Kurile–Kamchatka and Aleutian arcs based on regional tomography results. *Russian Geology and Geophysics (Geologiya i Geofizika)* 52 (6), 650–667.
- Kuwayama, Y., Hirose, K., Sata, N., Ohishi, Y., 2005. The pyrite-type high-pressure form of silica. *Science* 309, 923–925.
- Kuzmin, M.I., Yarmolyuk, V.V., Kravchinsky, V.A., 2010. Phanerozoic hot spot traces and paleogeographic reconstruction of the Siberian continent based on interaction with the African large lower shear velocity province. *Earth Sci. Rev.* 102 (1–2), 29–59.
- Kuzmin, M.I., Yarmolyuk, V.V., Kravchinsky, V.A., 2011. Phanerozoic within-plate magmatism of North Asia: absolute paleogeographic reconstructions of the African large low shear velocity Province. *Geotektonika* 45 (6), 415–438.

- Levin, B.V., Kim, Ch.U., Nagornykh, T.V., 2008. Seismicity of Priamurie and Priamurie in 1888–2008 [in Russian]. *Vestnik FEB RAS* (6), 16–22.
- Li, C., Van der Hilst, R.D., Engdahl, E.R., Burdick, S., 2008. A new global model for P wave speed variations in Earth's mantle. *Geochem. Geophys. Geosyst.* (G<sup>3</sup>) 9 (5). DOI:10.1029/2007GC001806.
- Litasov, K.D., Shatsky, A.F., 2016. Composition and Constitution of the Earth's Core [in Russian]. ISO SO RAN, Novosibirsk.
- Lyskova, E.L., 2014. Deep-Focus Earthquakes, in: *Problems of Geophysics*, Vol. 47 (Trans. St.-Petersburg State University, Issue 447) [in Russian]. St. Petersburg. Gos. Univ., St. Petersburg.
- Maruyama, S., 1994. Plume tectonics. *J. Geol. Soc. Japan* 100, 24–49.
- Meade, C., Jeanloz, R., 1991. Deep-focus earthquakes and recycling of water into the Earth's mantle. *Science* 252, 68–72.
- Meng, L., Ampuero, J.-P., Bürgmann, R., 2014. The 2013 Okhotsk deep-focus earthquake: Rupture beyond the metastable olivine wedge and thermally controlled rise time near the edge of a slab. *Geophys. Res. Lett.* 41, 3779–3785. DOI:10.1002/2014GL059968.
- Mück, L.A., Lattanzi, V., Thorwirth, S., McCarthy, M.C., Gauss, J., 2012. Cyclic SiS<sub>2</sub>: A New Perspective on the Walsh Rules. *Angewandte Chemie, Int. Ed.* 51 (15), 3695–3698.
- Ogawa, M., 1987. Shear instability in a viscoelastic material as the cause of deep focus earthquakes. *J. Geophys. Res. B, Solid Earth Planets* 92, 13,801–13,810.
- Pechersky, D.M., Didenko, A.N., Lykov, A.V., Tikhonov, L.V., 1993. Petro-magnetic model of the oceanic lithosphere. *Fizika Zemli*. No. 12, 29–45.
- Pushcharovsky, D.Yu., Oganov, A.R., 2006. Structural Transformations of Minerals in Deep Geospheres: A Review. *Crystallogr. Rep.* 51 (5), 767–777.
- Rodkin, M.V., Rundkvist, D.V., 2017. Geofluid Geodynamics. Application to Seismology, Tectonics, Processes of Ore and Oil-Genesis [in Russian]. Intellect, Moscow.
- Shestakov, N.V., Ohzono, M., Takashi H., Gerasimenko, M.D., Bykov, V.G., Gordeev, E.I., Chebrov, V.N., Titkov, N.N., Serovetnikov, S.S., Vasilenko, N.F., Prytkov, A.S., Sorokin, A.A., Serov, M.A., Kondratyev, M.N., Pupatenko, V.V., 2014. Modeling of coseismic crustal movements initiated by the May 24, 2013,  $M_w = 8.3$  Okhotsk deep focus earthquake, *Dokl. Earth Sci.* 457 (4), 976–981.
- Silvi, B., Savin, A., 1994. Classification of chemical bonds based on topological analysis of electron localization functions. *Nature* 371, 683–686.
- Tatevossian, R.E., Kosarev, L.G., Bykova, V.V., Matsievkii, S.A., Ulov, I.V., Aptekman Zh., Ya., Vakarchuk R.N., 2014. A deep-focus earthquake with  $M_w = 8.3$  felt at a distance of 6500 km. *Izvestiya. Phys. Solid Earth* 50 (3), 453–461.
- Turner, H.H., 1922. On the arrival of earthquake waves at the antipodes, and on the measurement of the focal depth of an earthquake, in: *Monthly Notices of the Royal Astronomical Society. Geophys. Suppl.*, Vol. 1, pp. 1–13.
- Van der Hilst, R., Engdahl, R., Spakman, W., 1993. Tomographic inversion of P and pP for aspheric mantle structure below the north-west Pacific region. *Geophys. J. Int.* 115, 264–302.
- Varga, P., Rogozhin, E.A., Shule, B., Andreeva N.V., 2017. A study of the energy released by great ( $M = 7$ ) deep focus seismic events with allowance for the  $M_w$  8.3 earthquake of May 24, 2013 in the Sea of Okhotsk, Russia. *Izvestiya. Phys. Solid Earth* 103 (3), 62–87.
- Voronina, E.V., 2016. Deep-Focus Earthquakes in the Sea of Okhotsk [in Russian]. Scientific Notes of Physical Department 3, 163902-1–163902-3.
- Wei, S., Helmberger, D., Zhan, Z., Graves, R., 2013. Rupture complexity of the  $M_w$  8.3 Sea of Okhotsk earthquake: Rapid triggering of complementary earthquakes? *Geophys. Res. Lett.* 40, 1–6.
- Yarmolyuk, V.V., Kuzmin, M.I., Vorontsov, A.A., Khomutova, M.Yu., 2013. West Pacific-type convergent boundaries: Role in the crust growth history of the Central Asian orogeny. *J. Asian Earth Sci.* 62, 67–78.
- Ye, L., Lay, T., Kanamori, H., Koper, K.D., 2013. Energy release of the 2013  $M_w$  8.3 Sea of Okhotsk earthquake and deep slab stress heterogeneity. *Science* 341, 1380–1384.
- Zhan, Z., Kanamori, H., Tsai, V.C., Helmberger, D.V., Wei, S., 2014. Rupture complexity of the 1994 Bolivia and 2013 Sea of Okhotsk deep earthquakes. *Earth Planet. Sci. Lett.* 385, 89–96.
- Zhao, D., Tian, Y., 2013. Changbai intraplate volcanism and deep earthquakes in East Asia: a possible link? *Geophys. J. Int.* 195, 706–724.
- Zhao, J., Pan, Z., Xu, B., Wang, X., 2014. The exceptions to the Walsh rules: Linear and cyclic structures of EX<sub>2</sub> (E = C, Si, Ge, Sn, Pb and X = O, S, Se). *Computat. Theor. Chem.* 1045, 22–28.
- Zharkov, V.N., 2013. Internal Structure of the Earth and Planets. Elementary Introduction to Planetary and Satellite Geophysics [in Russian]. Nauka i Obrazovanie, Moscow.
- Zonenshain, L.P., Kuzmin, M.I., 1993. *Paleogeodynamics* [in Russian]. Nauka, Moscow.
- Zyubina, T.S., 1998. Theoretical study of structure and stability of linear and cyclic isomers of silica, germanium, tin and lead dioxides. *Theoreticheskaya Neorganicheskaya Khimiya* 43 (2), 276–279.